B-branch electron transfer in reaction centers of Rhodobacter sphaeroides assessed with site-directed mutagenesis

Boer, A.L. de; Neerken, S.; Wijn, R. de; Permentier, H.P.; Gast, P.; Vijgenboom, E.; Hoff, A.J.

Photosynthesis Research **71:** 221–239, 2002.

Regular paper

B-branch electron transfer in reaction centers of *Rhodobacter sphaeroides* assessed with site-directed mutagenesis

Arjo L. de Boer[1], Sieglinde Neerken[1], Rik de Wijn[1], Hjalmar P. Permentier[1], Peter Gast[1,*], Erik Vijgenboom[2] & Arnold J. Hoff[1,†]

[1]*Department of Biophysics, Huygens Laboratory, Leiden University, P.O. Box 9504, 2300 RA Leiden, The Netherlands;* [2]*Leiden Institute of Chemistry, Gorlaeus Laboratories, Leiden University, P.O. Box 9504, 2300 RA Leiden, The Netherlands; *Author for correspondence (e-mail: gast@biophys.leidenuniv.nl; fax +31-71-5275819)*

Received 22 May 2001; accepted in revised form 7 December 2001

Key words: B-branch, electron transport, photosynthesis, *Rhodobacter sphaeroides*, site-directed mutagenesis

Abstract

Mutants of *Rhodobacter (Rba.) sphaeroides* are described which were designed to study electron transfer along the so-called B-branch of reaction center (RC) cofactors. Combining the mutation L(M214)H, which results in the incorporation of a bacteriochlorophyll, β, for H_A [Kirmaier et al. (1991) Science 251: 922–927] with two mutations, G(M203)D and Y(M210)W, near B_A, we have created a double and a triple mutant with long lifetimes of the excited state P* of the primary donor P, viz. 80 and 160 ps at room temperature, respectively. The yield of $P^+Q_A^-$ formation in these mutants is reduced to 50 and 30%, respectively, of that in wildtype RCs. For both mutants, the quantum yield of $P^+H_B^-$ formation was less than 10%, in contrast to the 15% B-branch electron transfer demonstrated in RCs of a similar mutant of *Rba. capsulatus* with a P* lifetime of 15 ps [Heller et al. (1995) Science 269: 940–945]. We conclude that the lifetime of P* is not a governing factor in switching to B-branch electron transfer. The direct photoreduction of the secondary quinone, Q_B, was studied with a triple mutant combining the G(M203)D, L(M214)H and A(M260)W mutations. In this triple mutant Q_A does not bind to the reaction center [Ridge et al. (1999) Photosynth Res 59: 9–26]. It is shown that B-branch electron transfer leading to $P^+Q_B^-$ formation occurs to a minor extent at both room temperature and at cryogenic temperatures (about 3% following a saturating laser flash at 20 K). In contrast, in wildtype RCs $P^+Q_B^-$ formation involves the A-branch and does not occur at all at cryogenic temperatures. Attempts to accumulate the $P^+Q_B^-$ state under continuous illumination were not successful. Charge recombination of $P^+Q_B^-$ formed by B-branch electron transfer in the new mutant is much faster (seconds) than has been previously reported for charge recombination of $P^+Q_B^-$ trapped in wildtype RCs (10^5 s) [Kleinfeld et al. (1984b) Biochemistry 23: 5780–5786]. This difference is discussed in light of the different binding sites for Q_B and Q_B^- that recently have been found by X-ray crystallography at cryogenic temperatures [Stowell et al. (1997) Science 276: 812–816]. We present the first low-temperature absorption difference spectrum due to $P^+Q_B^-$.

Abbreviations: A-branch – active electron transport branch; B-branch – inactive electron transport branch; β-mutant – L(M214)H; W_{M160}H-mutant – Y(M210)W/L(M214)H; DW_{M210}H-mutant – G(M203)D/Y(M210)W/L(M214)H; DH-mutant – G(M203)D/L(M214)H; DHW_{M260}-mutant – G(M203)D/L(M214)H/A(M260)W; P – primary electron donor; Q_A – secondary electron acceptor; *Rba.* – *Rhodobacter*; RC – reaction center

Introduction

The photosynthetic reaction center (RC) of the purple bacterium *Rhodobacter (Rba.) sphaeroides* is a membrane protein that consists of three protein subunits designated as L(ight), M(edium) and H(eavy) on the basis of their apparent molecular weights as determined by SDS-PAGE (Feher and Okamura 1978). The crystal structure of the *Rba. sphaeroides* RC has been solved (Allen et al. 1987a, b, 1988a; Ermler et al. 1994; McAuley-Hecht et al. 1998) and is currently known at a resolution of 2.6 Å. The protein provides a scaffold that binds several cofactors. One of the most striking features of the RC is that the redox cofactors form two branches, labelled A and B (Allen et al. 1988b; Hoff 1988), that are related by an approximately two-fold rotational symmetry axis perpendicular to the plane of the membrane. On the periplasmic side of the membrane, the two branches share a dimer of bacteriochlorophyll *a* molecules, which functions as the photo-oxidizable primary electron donor, P. This dimer is flanked by two symmetrically placed bacteriochlorophyll *a* monomers, B_A and B_B, each of which is followed by a monomeric bacteriopheophytin *a*, H_A and H_B, respectively, and by a ubiquinone UQ_{10}, Q_A and Q_B, respectively. The latter cofactors are located near the cytoplasm. A non-heme ferrous iron ion is situated between the two ubiquinones on the C_2 symmetry axis.

In spite of the fact that, *a prima facie*, both branches could be active in charge separation, only one of them, the active or A-branch, is actually used, as evidenced by the photobleaching of only H_A and not of H_B (Kirmaier et al. 1985a, b; Tiede et al. 1987; Aumeier et al. 1990). Thus:

$$PB_AH_AQ_AQ_B \rightarrow P^*B_AH_AQ_AQ_B \rightarrow$$
$$P^+B_A^-\,H_A\,Q_AQ_B \rightarrow P^+B_AH_A{}^-Q_AQ_B \rightarrow$$
$$P^+B_AH_AQ_A{}^-Q_B \rightarrow P^+B_AH_AQ_AQ_B{}^-.$$

An upper limit of 5% has been determined for electron transfer to H_B (Kirmaier et al. 1985b; Bixon et al. 1989; Aumeier et al. 1990; Woodbury et al. 1995). The factors controlling the branching of charge separation are not understood.Recent studies indicate that in principle both branches are accessible. Katilius et al. (1999) have shown that the yield of B-branch electron transfer could be enhanced by a mutation that results in the replacement of B_B by a bacteriopheophytin, Φ_B, with a higher redox midpoint potential. It is interesting to note that for RCs of *Chloroflexus aurantiacus,* which naturally posses a bacteriopheophytin at the position of B_B, a quantum yield for A-branch electron transfer of 1.0 was found (Volk et al. 1991).

Increased B-branch electron transfer was also found by Kirmaier et al. (1999), who introduced a lysine residue near B_B, which is likely to increase the redox potential of this pigment in its binding site. Alternatively, Heller et al. (1995) and Hartwich et al. (1997) observed that when electron transfer through the A-branch was slowed down, as evidenced by increased P^* lifetimes, B-branch charge separation was enhanced. However, several RC mutants with increased P^* lifetimes have been made for which no B-branch electron transfer has been reported. RCs with increased P^* lifetimes can be grouped in the following classes: (i) RCs with an increased P/P^+ midpoint potential, (ii) RCs with a decreased $B_A{}^-/B_A$ midpoint potential (or in which B_A has been replaced by a pigment with a lower midpoint potential), (iii) RCs with a decreased $H_A{}^-/H_A$ midpoint potential (or in which H_A has been replaced by a pigment with a lower midpoint potential), and (iv) RCs which are combinations of the classes (ii) and (iii). Several RC mutants of the first class have been constructed, but none of them shows B-branch electron transfer (Williams et al. 1992a, b; Stocker et al. 1992; Murchison et al. 1993; Lin et al. 1994; Tang et al. 1999). This is not surprising, since changing the P/P^+ midpoint potential equally affects the free energies of charge-separated states in the A- and the B-branch. Since electron transfer through the A-branch is activationless, a small change in the driving force, ΔG, will have but little effect on its rate k_A. The same change in driving force may affect k_B more, depending on the Marcus regime (normal, activationless, inverted). The results of Williams et al. (1992a, b), however, suggest that k_B is not significantly enhanced.

RCs of the second category were studied by Hartwich et al. (1997, 1998). They replaced B_A with vinyl-bacteriochlorophyll, which has a midpoint potential that is *lower* by ~130 mV *in vitro*. This pigment exchange resulted in an increase of the P^* lifetime from 3 to 30 ps at 290 K, and from 2 to 300 ps at 90 K. The increase of the P^* lifetime was accompanied by enhanced electron transport through the B-branch, but no quantitative data was given and the results were only reported in abstract form (Hartwich et al. 1997, 1998). RCs of the third type have been made by mutagenesis (Robles et al. 1990; Kirmaier et al. 1991; Heller et al. 1996) and by exchange of H_A by pigments with different redox properties (Huber et al. 1995; Meyer and Scheer 1995; Schmidt et al. 1995;

Kennis et al. 1997a). No B-branch electron transport was reported for these RCs. B-branch electron transfer in RCs of class (iv) has been demonstrated (Heller et al. 1995) in RCs of *Rba. capsulatus* that contain two mutations: The first mutation probably lowers the B_A^-/B_A midpoint potential (makes it more negative) and the second mutation lowers the primary acceptor's midpoint potential. A single-point mutation does not induce significant B-branch electron transfer, whereas upon double or triple mutation the yield of $P^+H_B^-$ formation is 15% (Heller et al. 1995). It has been suggested that absorption changes in the bacteriopheophytin Q_x region due to the formation of a small amount of $P^+H_B^-$, may be masked by the relatively large absorption changes due to the formation of $P^+H_A^-$ (Heller et al. 1995). Such small absorption changes then could be detected by including the L(M212)H mutation, since this mutation removes absorption changes due to the formation of $P^+H_A^-$ from the bacteriopheophytin Q_x region.

The guiding principle of the above studies was that slowing down A-branch electron transfer *without affecting the B-branch* would lead to enhanced B-branch electron transfer. Using this principle as a working hypothesis, we have constructed class (iv) RCs of *Rba. sphaeroides* with a much longer P* lifetime than reported so far. We have used the mutation L(M214)H to replace H_A with a bacteriochlorophyll molecule, which has a lower midpoint potential. This mutation corresponds to the mutation L(M212)H in the *Rba. capsulatus* RCs used by Heller et al. (1995) (the so-called β-mutant). We used the mutation Y(M210)W rather than G(M203)D to destabilize the state $P^+B_A^-$. The mutation Y(M210)W causes an increase of the P* lifetime from 3 to 36 ps (Shochat et al. 1994), considerably longer than the P* lifetimes of 6 and 9 ps that have been reported to result from the mutations G(M201)D and G(M203)D in the RCs of *Rba. capsulatus* (Heller et al. 1995) and *Rba. sphaeroides* (Williams et al. 1992a), respectively. The new RC, containing the mutations L(M214)H and Y(M210)W, was expected to have a long P* lifetime and to have significant B-branch photochemistry. We have also made an RC triple mutant by combining mutation L(M214)H with both the mutations G(M203)D and Y(M210)W to further destabilize the state $P^+B_A^-$ and obtain an RC with an even longer P* lifetime. Thus, the following mutants were constructed (the labels used in this article are in parentheses):

L(M214)H (β-mutant)
Y(M210)W / L(M214)H (W_{M210}H-mutant)
G(M203)D / Y(M210)W / L(M214)H (DW_{M210}H-mutant)
G(M203)D / L(M214)H (DH-mutant)
G(M203)D / L(M214)H / A(M260)W (DHW_{M260}-mutant).

In spite of the strongly increased P* lifetimes and corresponding reduced yields for the formation of $P^+Q_A^-$ for both the double and triple mutant, no appreciable electron transfer to H_B was observed in either mutant. We conclude that the lifetime of P* as a measure of A-branch activity is not a governing factor inducing B-branch electron transfer.

To study *direct* photoreduction of Q_B and subsequent *direct* $P^+Q_B^-$ charge recombination (i.e. photoreduction and recombination in which only B-branch cofactors are involved), a triple mutant of *Rba. sphaeroides* was designed combining the G(M203)D and L(M214)H mutations with the A(M260)W mutation, which leads to the exclusion of Q_A from the RC (see Figure 1). In our triple mutant β is the final electron acceptor in the A-branch since the third mutation excludes Q_A from the RC. Because the triple mutant only has mutations near the A-branch, the energetics of the B-branch in this mutant are presumably unaltered and therefore represent a wild-type B-branch. $P^+Q_B^-$ formation via the B-branch at room temperature has recently been described for a similar RC mutant of *Rba. capsulatus* (Laible et al. 1998). In contrast to the room temperature work by Laible et al. (our studies) on the DHW_{M260} mutant deal with $P^+Q_B^-$ formation at cryogenic temperatures. Evidence is presented that B-branch electron transfer occurs in the triple mutant both at room temperature and at cryogenic temperatures, leading to the formation of $P^+Q_B^-$. Furthermore, we present the first absorption difference spectrum recorded for $P^+Q_B^-$ formation at 20 K. The yield of $P^+Q_B^-$ formation following a saturating laser flash at 20 K, however, was only a few percent. This state did not photoaccumulate under continuous illumination at 20 K.

Materials and methods

Bacterial strains and growth conditions

The *Rba. sphaeroides* strain ΔLM1 (Paddock et al. 1989), in which the wildtype *pufM* gene and most

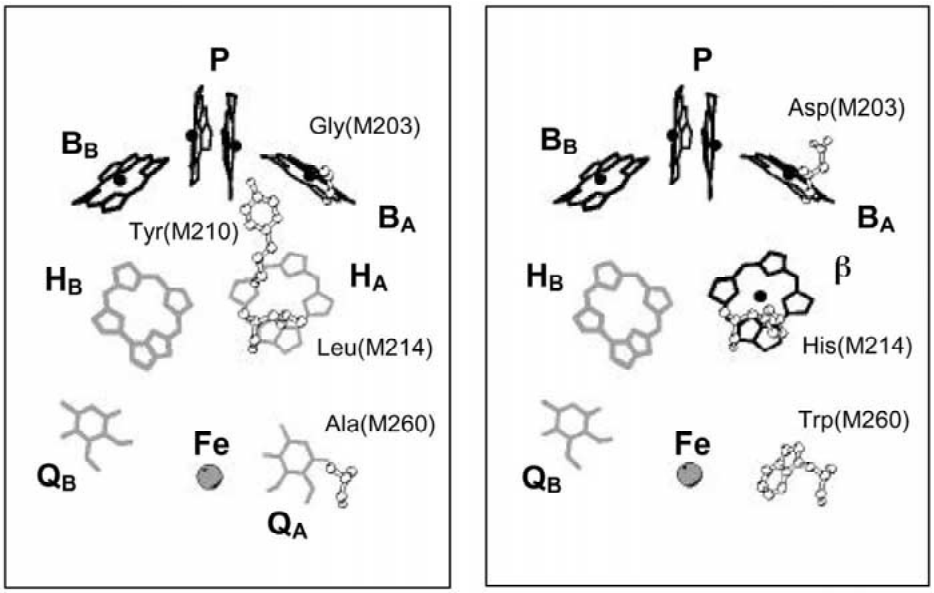

Figure 1. Schematic representations of the cofactors in wildtype RCs (left) and DHW_{M260} RCs (right). Amino acid residues that have been mutated are also shown. For clarity, only the porphyrin rings of the bacteriochlorphylls and bacteriopheophytins are shown. For the same reason, the carotenoid and the isoprenoid tails of the quinones have been omitted. See text for details. The structures have been drawn after Ermler et al. (1994), using the Molscript program (Kraulis 1991).

of the *pufL* gene have been replaced by a kanamycin resistance cassette, was used for expression of the plasmid encoded *puf* operon. Pseudo-wildtype RCs with an engineered poly-histidine tag were isolated from the deletion strain ΔLM1 complemented with the plasmid pRKENBH. Plasmid pRKENBH is a derivative of pRKENB (Paddock et al. 1989) in which a *Bam*HI site has been introduced immediately after the stop codon of *pufM* (Williams et al. 1992a). We have inserted seven codons (CAC) for histidine 5′ of the stop codon of *pufM* in order to facilitate RC purification. RCs from the resulting strain do not have the Ala→Ser mutation at position M304 that is present in RCs isolated from the analogous strain SMpHis (Goldsmith and Boxer 1996), nor does the LH1 α-peptide have the His→Glu mutation at position 32.

E. coli JM109 (*recA*1*supE*44*endA*1*hsdR*17 (r_k^-, m_k^+)*gyrA*96*relA*1*thi* Δ*(lac-proAB)* [F′, *traD36 proAB*$^+$ *lacI*^{q} *lacZ*Δ*M15*]) (Yanish-Perron et al. 1985) was used as a host during plasmid construction. *E. coli* S17-1 (*thi pro hsdR*$^-$ *hsdM*$^+$ *recA* Tp^R Sm^R RP4-2 (Tc::Mu km::Tn7)) (Simon et al. 1983) was used for introduction of plasmids into ΔLM1 via conjugation.

E. coli strains were grown in Luria Broth with appropriate antibiotics. *Rba. sphaeroides* strains were routinely grown under semi-aerobic/dark conditions in YCCS medium [YCC medium (Sistrom 1977) supplemented with 0.3% succinic acid]. All *Rba. sphaeroides* strains were grown in the presence of kanamycin; for strains carrying pRKENBH or its mutant derivatives tetracycline was also included. For *E. coli* antibiotic concentrations were: Ampicillin, 100 μg/ml, kanamycin 25 μg/ml, tetracycline, 12 μg/ml. For *Rba. sphaeroides*, antibiotic concentrations were: Kanamycin, 25 μg/ml, tetracycline, 2.5 μg/ml.

Photosynthetic growth assays were performed on plates in an anaerobic jar (Oxoid Ltd, Basingstoke, UK) placed in a climatized room at 30 °C. An anaerobic atmosphere was created using an AnaeroGen sachet (Oxoid Ltd, Basingstoke, UK). Light was provided by six tungsten light bulbs at a distance of 30 cm from the jar. The *pufLM* deletion strain ΔLM1 was used as a negative control, the same deletion strain complemented with plasmid pRKENBH (the wildtype) was used as a positive control. Under the conditions tested, growth of the wildtype became visible after 3–4 days. No growth was visible for the deletion strain, even after a prolonged incubation of up to 14 days.

Construction of mutants

DNA manipulations were carried out according to Sambrook et al. (1989). Restriction enzymes were ob-

tained commercially and used as indicated by the suppliers. DNA fragments were isolated from gels using the Gene-Clean II kit (Bio101, Vista, California).

Site-directed mutations in the *pufM* gene were made by the following codon changes: GGT→GAC (M203 g→D), TAC→TGG (M210 Y→W), CTG→CAC (M214 L→H) and GCC→TGG (M260 A→W). The mutations were introduced by PCR-methods (Landt et al. 1990) using the proof-reading-proficient Vent DNA polymerase (New England Biolabs, Beverly, Massachusetts). PCR fragments were cloned into the pTZ19R phagemid (USB, Cleveland, Ohio). Single-stranded DNA from the resulting chimeras was sequenced through the region of interest by Base-Clear (Leiden, The Netherlands). The *Bam*HI-*Xho*I fragment in pRKENBHSm, which contains a streptomycin resistance cassette inserted in the *Nco*I site of the *pufM* gene for screening purposes, was exchanged with the fragments containing the mutations. The resulting plasmids were introduced into *E. coli* S17-1 and shuttled into the *Rba. sphaeroides* deletion strain ΔLM1 via conjugation essentially as described by Paddock et al. (1989).

Cell growth and isolation of reaction centers

Photosynthetic growth was seen only for the wildtype. A few revertants or suppressor mutants were then found for the single L(M214)H mutant. No growth at all was observed for the $W_{M210}H$ double mutant (the DH mutant was not tested) and the triple mutants, nor for the *pufLM* deletion strain ΔLM1. As a precaution to avoid longer-term photosynthetic pressure that might lead to the accumulation of revertants or suppressor mutants, *Rba. sphaeroides* strains harboring mutant *pufM* genes were grown under semi-anaerobic/dark conditions.

The pseudo-wildtype was grown under the same conditions for reasons of comparability. Cultures grown aerobically in YCCS medium for 3–4 days were diluted 1:50 in 2 l Erlenmeyer flasks containing 1 l YCCS medium. These flasks were shaken for approximately 50 h at 200 rpm in a gyrotary shaker at 30 °C. Cells were disrupted by sonication. RCs with an engineered poly-histidine tag were isolated from the deletion strain ΔLM1 complemented with the plasmid pRKENBH according to Goldsmith and Boxer (1996) with the following modifications. Pro-Bond Resin (Invitrogen B.V., Leek, The Netherlands) containing Ni^{2+} ions was used to bind the RCs by their poly-histidine tag. Chromatophores were stirred with this resin for 1 h at room temperature in the presence of LDAO (0.5%) and imidazole (5 mM). For the second purification step Poros 50 HQ (PerSeptive Biosystems, Framingham, Massachusetts) was used as anion exchanger. An EDTA-containing buffer (TL: 10 mm Tris–HCL pH 8.0, 1 mm EDTA, 0.1% LDAO) was used during washing and elution. Purified RCs were dialyzed against TL-buffer and concentrated over a 100 kDa Amicon filter to an OD_{800} of 50–100 per centimeter. The yield was approximately 10 mg protein per liter of cell culture for both wildtype and mutants. The Q_B content in the samples was determined essentially as described by Okamura et al. (1982) and found to be less than 25%.

Steady-state spectroscopy

Steady-state absorption spectroscopy was performed using a single-beam spectrophotometer equipped with modulated measuring light (Otte 1992). Glycerol was added to a final concentration of 67% v/v to all samples used in low-temperature experiments. Photoaccumulation of $P^+Q_B^-$ at 6 K was studied by monitoring the bleaching of the P band near 890 nm under continuous illumination with light from a xenon lamp at an intensity of approximately 1 W cm^{-2}. UQ_{10} was added in 10-fold excess to the RCs to ensure full occupation of the Q_B site.

Picosecond transient absorption spectroscopy

Time-resolved transient absorption difference measurements at room temperature were performed with a home-built amplified dye laser system with continuum generation and optical multichannel analyzer (OMA) detection, operating at 10 Hz, described by Kennis et al. (1996, 1997b). The time resolution was 600 fs. Excitation pulses were obtained by amplification of the continuum in a dye cell (LDS 867, Exciton). Excitation was in the absorption band of the primary donor at 865 nm. Wavelengths shorter than 850 nm were cut off with an RG850 filter (Melles Griot). Pump and probe pulses were polarized parallel to each other. The samples contained 5 mm ortho-phenantroline or 0.5 mm terbutryn to inhibit $P^+Q_B^-$ formation and were kept in a moving cuvette (optical pathway: 1 mm) in order to avoid accumulation of photo-oxidized P. The absorbance was adjusted to 1 per mm at the wavelength of interest. Approximately 5–10% of the P absorption band was bleached per laser pulse.

Charge recombination and yield of $P^+Q_B^-$

Formation and recombination of $P^+Q_B^-$ at room temperature were studied by monitoring the bleaching of the P band near 865 nm following subsaturating filtered flash light provided by a xenon flash lamp. A home-built single-beam spectrophotometer (Visser 1975; Shochat et al. 1995) was used to generate and record the kinetic data. The same apparatus was used to determine the yield of $P^+Q_B^-$ formation. A 10-fold excess of UQ_{10} was added to the RCs to ensure full occupation of the Q_B site. Subsaturating light from a tungsten halogen lamp filtered by an 860 nm interference filter was used to excite the Q_y band of P at 865 nm. The amplitude of the resulting bleaching of the Q_x band of P near 600 nm was measured and plotted as a function of the illumination time for samples of wildtype and mutant RCs with identical absorptions at 865 nm. The quantum yield for $P^+Q_B^-$ formation in DHW_{M260} RCs was determined by comparing for wildtype and mutant RCs the slopes at zero-time of the bleachings at 600 nm obtained under condition of unsaturating illumination, with the assumption of a 100% quantum yield for $P^+Q_B^-$ formation in wildtype RCs.

Formation and charge recombination at cryogenic temperatures were measured using a different single-beam spectrophotometer as described by Franken (1997). Saturating excitation flashes were provided by a Q-switched, frequency-doubled Nd-YAG laser (532 nm).

EPR measurements

The EPR measurements were performed with a home-built phase-sensitive homodyne combined pulsed and cw-EPR spectrophotometer (Bosch 1995; Dzuba et al. 1996).

Results

Absorption spectra

Low temperature absorption spectra of wildtype and the various mutant RCs are shown in Figure 2. The spectra of the double and triple mutants are similar to that of the β-mutant (Kirmaier et al. 1991), except for small (2–4 nm) shifts of the main accessory bacteriochlorophyll band. In all five mutants, the band of H_A is replaced by the Q_y β-BChl band while the intensity of the Q_y-band of bacteriopheophytin at 760 nm is decreased. The position of the β-band differs considerably for the various mutants, ranging between 773 and 784 nm. The large difference between the DH (775 nm) and the DHW_{M260} (784 nm) mutants must be due to the A(M260)W mutation. The effect of the G(M203)D mutation is most clearly seen in the DH mutant, in the region where the accessory bacteriochlorophylls have their Q_y absorption, between 790 and 820 nm. In this mutant the absorption maxima of B_A and B_B (799 and 814 nm, respectively) have separate peaks, in contrast to the wildtype where B_B appears as a shoulder (812 nm) of the B_A band (800 nm). This is in accordance with the spectra at 77 K published for the G(M203)D single mutant (Williams et al. 1992a), though the effect seen in our DH mutant at 6 K is more pronounced. The absorption spectrum at 77 K for the corresponding mutant of *Rba. capsulatus*, G(M201)D/L(M212)H, does not show separate peaks due to B_A and B_B (Heller et al. 1996). The splitting observed in the DH mutant is no longer seen in the DHW_{M260} triple mutant, presumably because of the A(M260)W mutation, which is present in the DHW_{M260} but not in the DH mutant. This is another indication that the A(M260)W mutation affects the Q_y absorption region of the bacteriochlorophylls B_A, B_B and β.

The Q_x bands of the bacteriopheophytins of the wildtype, which overlap at room temperature, are clearly resolved into two bands at 533 nm (H_B) and at 547 nm (H_A), respectively, at low temperature. In the mutants only one peak, of H_B, is observed at 533 nm at low temperature, due to the replacement of H_A by β.

Picosecond transient absorption difference spectroscopy

Time-resolved absorption difference spectra at several delay times of wildtype, $W_{M210}H$ and DHW_{M260} mutant RCs in the absorption band of P near 865 nm at room temperature are shown in Figure 3 (excitation in the P-band). Similar data (not shown) were obtained for the other mutants. Absorption changes in this wavelength region are due to ground-state bleaching of the 865 nm band together with stimulated emission of P* between 870 and 1000 nm. As in wildtype RCs the stimulated emission disappears as P* decays. For the $W_{M210}H$ and $DW_{M210}H$ mutants, the decay of the stimulated emission averaged between 930 and 940 nm was fitted with a single exponential and a constant component (Figure 4). A time constant of 80 ps was found for the $W_{M210}H$ mutant and a time constant of

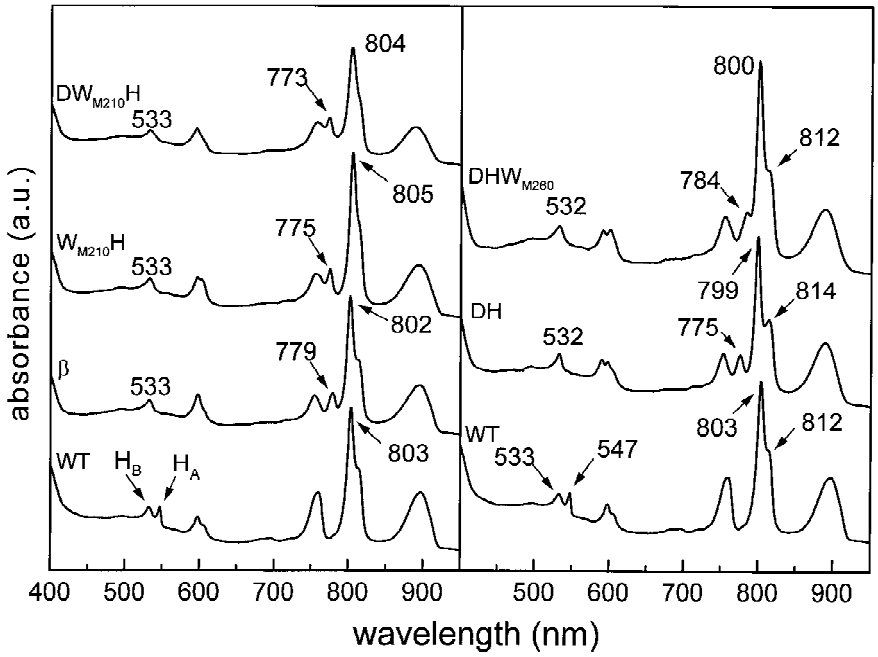

Figure 2. Absorption spectra of wildtype and mutant RCs at 6 K. For the labels of the mutants see text.

160 ps for the $DW_{M210}H$ mutant. There is no evidence for a fast component in the P* decay of either mutant (Figure 4, insets).

The long P* decay times imply a very slow charge separation. There is a significant decrease in the amplitude of the long-time bleaching of the 865 nm band compared to that of wildtype RCs (Figure 3), which is interpreted as a diminished yield of long-lived charge-separated states in the mutants (on the time scale of the measurements). This lower yield could be caused by direct deactivation of P* to the ground state and/or by enhanced recombination of charge-separated states involving B_A or β. Fits of the bleachings, averaged between 930 and 940 nm, with single exponentials yielded time constants of about 200 ps for both the $W_{M210}H$ and the $DW_{M210}H$ mutant (Figure 4, lower and middle panel). Recovery was 50 and 70%, respectively, of the P-bleaching in the initial spectra compared to that measured at a delay of 1.9 ns (Figure 3). This means approximately 50 and 30% yield of $P^+Q_A^-$ formation for the $W_{M210}H$ double and $DW_{M210}H$ triple mutant, respectively.

The decay kinetics of the stimulated emission from P* in the DHW_{M260} mutant are shown in Figure 4, upper panel. A single exponential fit of the decay between 920 and 930 nm was not satisfactory for both the DHW_{M260} and the DH (not shown) mutants. A double exponential fit of the DHW_{M260} decay yielded lifetimes of 2.5 $\pm$ 1 (40%) and 36 $\pm$ 5 (60%) ps. The average time constant of 23 ps (obtained by averaging the lifetimes using their relative amplitudes as weight factors) is somewhat larger than the 15 ps lifetime which was obtained in a monoexponential fit for the *Rba. capsulatus* mutant G(M201)D/L(M212)H (Heller et al. 1995). Since no more than 5% B-branch electron transfer occurs in the DHW_{M260} mutant (see below) and electron transfer to Q_A is blocked [Q_A is absent due to the A(M260)W mutation (Ridge et al. 1999; McAuley et al. 1999, 2000)], P* decays mainly by charge separation through the A-branch. Significant recovery of the ground state of P occurs during the P* lifetime, as evidenced in Figure 3. Ground state recovery was also found for the*Rba. capsulatus* mutant G(M201)D/L(M212)H (Heller et al. 1995) with a yield of 15%. In the DHW_{M260} mutant ground state recovery continues after the stimulated emission has disappeared. In this mutant, the final charge-separated state in the A-branch is $P^+\beta^-$. Apparently considerable ground state recovery of P occurs due to charge recombination of $P^+\beta^-$ (or $P^+B_A^-$, which may be in equilibrium with $P^+\beta^-$). In contrast, essentially no decay of the bleaching of the P band near 865 nm is seen for wildtype RCs (Figure 3) due to the fact that $P^+Q_A^-$ is formed with a yield of $\sim$100% and does

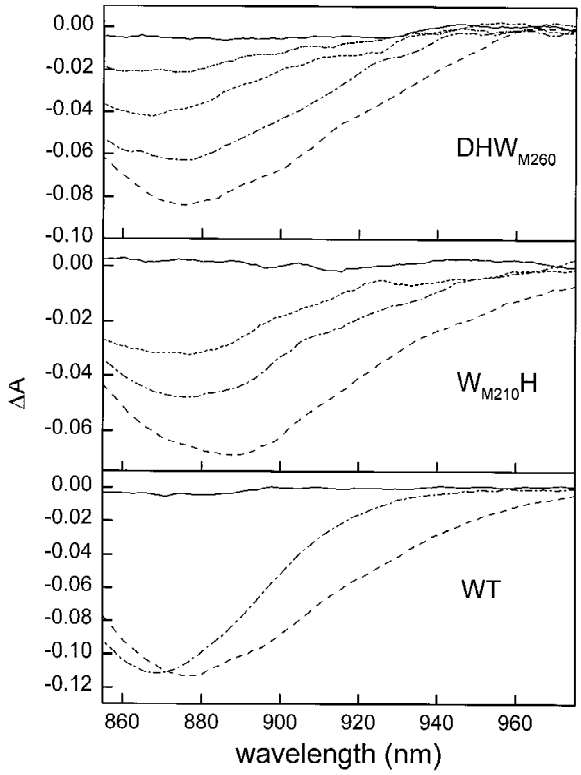

Figure 3. Transient difference spectra at the long wavelength absorption band of P at room temperature. Upper panel: DHW_{M260} RCs at several delay times: Before excitation (solid), 1 ps (dashed); 50 ps (dash-dotted); 300 ps (short-dashed) 1.9 ns (short-dash-dotted). Middle panel: $W_{M210}H$ RCs at several delay times: Before excitation (solid), 1.4 ps (dashed); 90 ps (dash-dotted); 1.9 ns (short-dashed). Lower panel: wildtype RCs before excitation (solid), at 1.5 ps (dashed) and at 1.5 ns (dash-dotted). The absorbance was 1 at 865 nm.

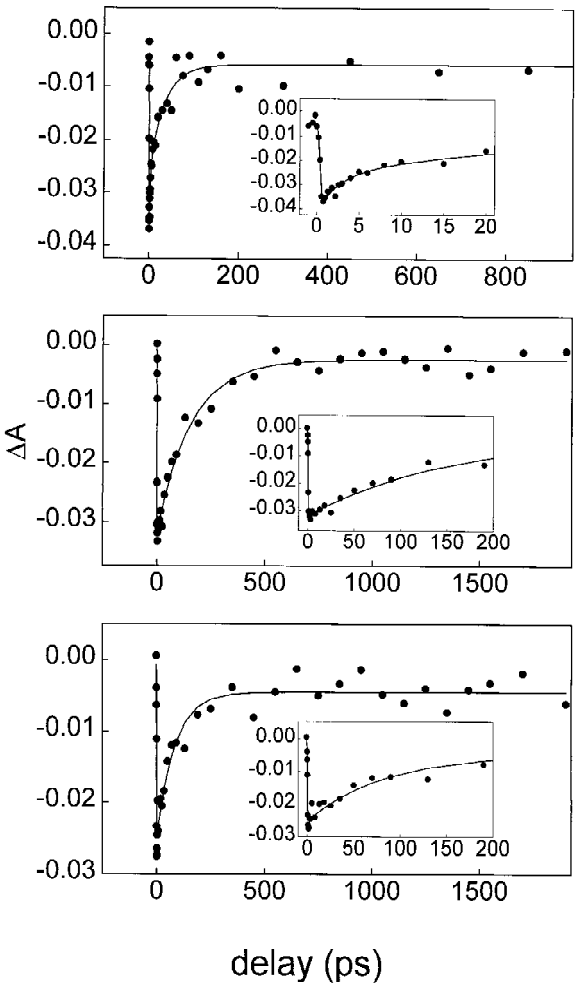

Figure 4. Kinetics of P* decay at room temperature. Upper panel: the DHW_{M260} mutant, averaged between 920 and 930 nm, and a biexponential fit with time constants of 2.5 and 36 ps and a constant component. The inset shows data and fit during the first 20 ps. Middle and lower panel: the $DW_{M210}H$ and $W_{M210}H$ mutants, respectively, averaged between 930 and 940 nm, and fits with a single exponential with time constant of 160 and 80 ps, respectively, and a constant component. The insets show data and fits of the first 200 ps.

not decay on the nanosecond time scale. No further P recovery was observed in the G(M201)D/L(M212)H mutant of *Rba. capsulatus* after disappearance of P* (Heller et al. 1995).

Figure 5 shows absorption changes in the Q_x region of the bacteriopheophytins for the $W_{M210}H$ and DHW_{M260} mutants and wildtype RCs, under conditions where approximately 10% of the P absorption band was bleached. For the mutants transient absorption changes near 530 nm, the position of the Q_x absorption of H_B, reflect B-branch charge separation at room temperature. In wildtype RCs H_A and H_B have overlapping Q_x absorption bands, and the time-resolved spectrum shows a bleaching at 545 nm due to the reduction of H_A. We estimated the amount of H_B bleached in mutant RCs by comparing the magnitude of the absorption changes near 530 nm at several delay times (attributed to $P^+H_B^-$ formation) with the magnitude of the bleaching observed near 545 nm (due to $P^+H_A^-$ formation) in wildtype RCs at a delay time of 10 ps (3 times the lifetime of P*), other conditions being equal. It was assumed that the oscillator strengths for H_A and H_B are similar and that $P^+H_A^-$ is formed with quantum yield of 100% in wildtype RCs. With the signal-to-noise ratio in our experiments, an upper limit of 5-10% was estimated for the yield of $P^+H_B^-$ in the double or triple mutant (Figure 5). This yield is significantly less than the yield of ∼15% that has

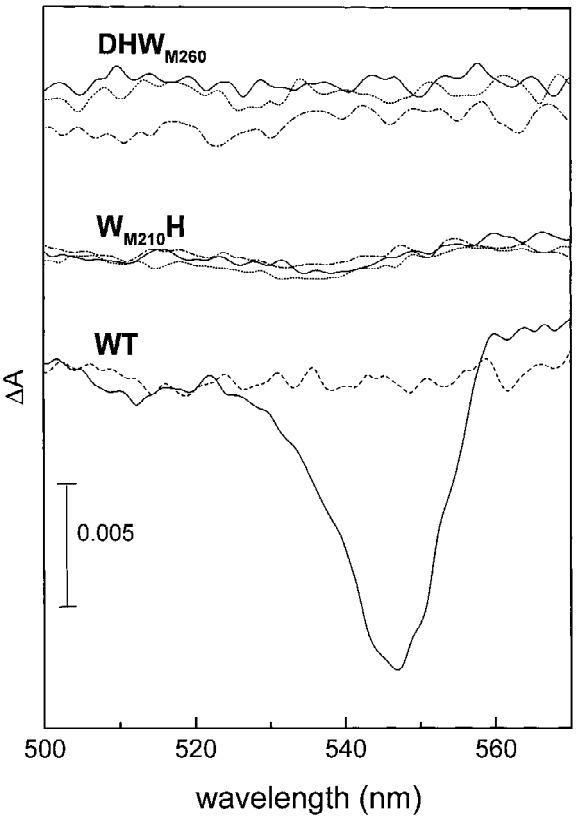

Figure 5. Transient difference spectra in the region of the Q_x bands of H_A and H_B. Wildtype RCs: before excitation (dashed) and at a delay time of 10 ps (solid); $W_{M210}H$ mutant RCs: delay times of 40 (solid), 100 (dotted) and 250 ps (dash-dotted); DHW_{M260} mutant RCs: delay times of 20 ps (solid), 100 ps (dotted) and 500 ps (dash-dotted). The absorbance was 1.0 at 530 nm. Approximately 10% of the P-absorption band was bleached per laser pulse. Similar results (not shown) were obtained for the $DW_{M210}H$ mutant.

been reported for the corresponding *Rba. capsulatus* DH mutant (Heller et al. 1995).

(Milli)second absorption difference spectroscopy

With the aim to investigate B-branch electron transfer to Q_B in the DHW_{M260} mutant, we have carried out flash-induced absorption spectroscopy between 700 and 920 nm on a (milli)second timescale, both at room temperature and at cryogenic temperatures (Figures 6–8). $P^+Q_A^-$ and $P^+Q_B^-$ are the only states known in the RC which fulfill the requirement of corresponding long lifetime. Since the DHW_{M260} mutant does not contain Q_A, the absorption changes are ascribed to the decay of $P^+Q_B^-$.

In Figure 6 decay kinetics at room temperature at the absorption band of P near 865 nm are shown for wildtype and DHW_{M260} RCs. For both types of RCs two traces are shown. One trace was obtained in the presence of excess UQ_{10}, ensuring a (nearly) full occupation of the Q_B site. The second trace was obtained in the presence of terbutryn, a well-known competitive inhibitor of Q_B, which inhibits $P^+Q_B^-$ formation. For wildtype RCs in the presence of UQ_{10}, the decay kinetics are dominated by recombination from $P^+Q_B^-$, which occurs with a time constant of approximately 1 s (Okamura et al. 1982; Kleinfeld et al. 1984b). In the presence of terbutryn, $P^+Q_A^-$ is the final charge-separated state; it decays with a time constant of ~100 ms (Kleinfeld et al. 1984b). Signals obtained for the DHW_{M260} mutant were much smaller. A yield of 5% was determined for $P^+Q_B^-$ formation. In the DHW_{M260} mutant the decay kinetics in the presence of UQ_{10} are ascribed to decay of $P^+Q_B^-$, as in wildtype RCs. The decay, however, is much slower than in wildtype RCs. A biexponential fit yields time constants of 4.5 and 57 s with equal amplitudes. In the presence of terbutryn the signal has almost completely vanished (the small residual signal is attributed to $P^+Q_B^-$ decay in a small fraction of the RCs still containing Q_B). This is due to the fact that under these conditions neither $P^+Q_A^-$ nor $P^+Q_B^-$ can be formed. These results show (i) that absorption changes on the time scale of seconds in the DHW_{M260} mutant are associated with the state $P^+Q_B^-$, (ii) that there is no other acceptor in the RC that can give rise to long-lived charge-separated states involving P, and (iii) that $P^+Q_B^-$ signals are not due to adventitious reduction of excess UQ_{10} by P^*.

Absorption changes were observed in the DHW_{M260} triple mutant even at 10 K, suggesting that $P^+Q_B^-$ is formed even at this low temperature. As mentioned before, no $P^+Q_A^-$ formation is expected since no Q_A is present in the mutant due to the A(M260)W mutation. Absorption difference kinetics at 20 K were obtained for wavelengths between 700 and 920 nm (Figure 7). The kinetics showed biexponential behaviour with time constants of 0.6 s and 2.7 s with equal amplitudes. The average time constant of 1.7 s is more than an order of magnitude smaller than the average time constant obtained at room temperature. For each wavelength, the absorption changes were averaged between 100 and 500 ms and used to construct a $P^+Q_B^-$ absorption difference spectrum (Figure 8). Approximately 3% of the P-band was bleached in a single, saturating flash. In a similar way, kinetics were obtained for the DH mutant in the presence of terbutryn. Under these conditions, only $P^+Q_A^-$ can

be formed. An absorption difference spectrum was obtained by averaging the data between 2 and 5 ms (Figure 8).

Near 890 nm, a bleaching of the P band is observed. Changes near 760 nm in the DH and DHW_{M260} mutant can be attributed to H_B only since H_A has been replaced with β. Changes near 780 nm in the DH and DHW_{M260} mutant are due to a shift of this β chromophore. Changes near 800 nm are due to bandshifts of B_A and/or B_B. In the difference spectra for the DH and the DHW_{M260} mutant, the bandshift of B_A is characterized by a peak at 795 nm and a trough at 800 nm. The bandshift of B_B causes a peak at 804 nm and a trough at 816 nm in the spectrum of the DH mutant, whereas a peak at 807 nm and a trough at 819 nm are found for the DHW_{M260} mutant. In the DHW_{M260} mutant, the bandshift of B_B is dominant. Due to its position in the B-branch, B_B may experience a stronger electric field from the state $P^+Q_B^-$ than from the state $P^+Q_A^-$.

As mentioned, approximately 3% of the P-band was bleached in a single, saturating flash at 20 K. We have tried to photo-accumulate the $P^+Q_B^-$ state under continuous illumination at cryogenic temperatures. Under these conditions, the P band in the absorption spectrum of wildtype RCs is fully bleached. For DHW_{M260} RCs, however, only a few percent of the P band was bleached. No signals were found for Q_B^- either, using EPR spectroscopy at liquid nitrogen temperatures. These results indicate that $P^+Q_B^-$ accumulation does not occur at cryogenic temperatures.

Discussion

Absorption spectra

The absorption spectrum at room temperature of the L(M214)H mutant (β-mutant) with an engineered poly-histidine tag is identical to the spectrum published previously for the same mutant without the poly-histidine tag (Kirmaier et al. 1991) (not shown). At low temperatures, the most striking differences compared to wildtype RCs are the absence of the 545 nm peak of H_A and the appearance of a new band at 779 nm, both caused by the replacement of H_A by β.

In the low temperature absorption spectra of the double mutant $W_{M210}H$ and the triple mutant $DW_{M210}H$, the characteristic features of the single mutants are combined. On the one hand there is a redshift of the accessory bacteriochlorophyll peak from 803 to 806 nm, a feature characteristic of the Y(M210)W mutant (Shochat et al. 1994). On the other hand the peak of H_A at 545 nm is absent and the β Q_y-band is blueshifted from 779 to 775 nm in the double and triple mutants. For the DH and DHW_{M260} mutants of the *Rba. sphaeroides* RC the β Q_y-band is located at 775 and 784 nm, respectively.

The variability of the absorption maximum of the β Q_y-band may be due to differences in the histidine-Mg bond, differences in the conformation of the macrocycle or different interactions with the other pigments in the RC in the respective mutants. These differences must also be responsible for the small amplitude of the β Q_y-band compared to those of the B_A and B_B Q_y-bands. Diffraction data on the L(M214)H mutant, collected to 3.3 Å resolution, suggests that there may be some flexibility in the conformation of the macrocycle (Chirino et al. 1994). The Q_x peak wavelength of the β pigment is not affected by the various mutations. Addition of the A(M260)W mutation to the G(M203)D and L(M214)H mutations of the DH mutant, yielding the DHW_{M260} mutant, causes a strong redshift of the β Q_y band from 775 to 784 nm. A much smaller redshift of the Q_y-band due to both H_A and H_B from 757 to 759 nm at room temperature was observed for the A(M260)W single mutant (Ridge et al. 1999).

When comparing wildtype and G(M203)D RCs at 77 K, the band at 800 nm and its shoulder near 810 nm are more resolved in the mutant than in the wildtype (Williams et al. 1992a). This effect is not visible in our triple mutant, probably due to the redshift from 803 to 806 nm caused by the Y(M210)W mutation.

P lifetimes and ground state recovery*

The time-resolved absorption difference spectra of the $W_{M210}H$ and $DW_{M210}H$ mutant show features that are different from both wildtype and β-type RCs of *Rba. sphaeroides* (Kirmaier et al. 1985a, b, 1991); see Table 1.

Decay of the stimulated emission occurs with time constants of 80 and 160 ps at room temperature for the $W_{M210}H$ and $DW_{M210}H$ mutants, respectively. These time constants are approximately 25 and 50 times larger than the time constant found for wildtype RCs (3 ps). They are also larger than found for each of the single mutants (Kirmaier et al. 1991; Shochat et al. 1994) (see Table 1), suggesting that the individual mutations cooperate to yield a long P* lifetime.

As mentioned, the mutation L(M214)H results in the incorporation of a bacteriochlorophyll molecule

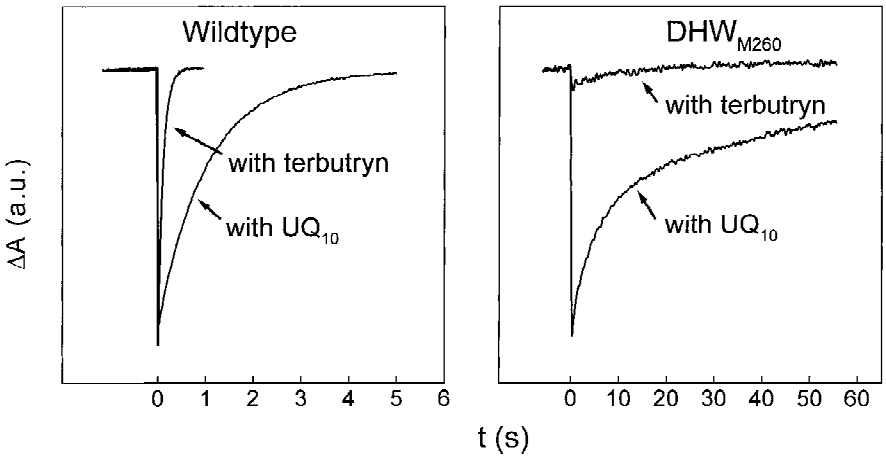

Figure 6. Charge recombination kinetics at 865 nm at room temperature in wildtype and DHW_{M260} RCs. Note the different time scales. The amplitudes of the traces obtained for DHW_{M260} RCs are actually 20-fold smaller than those obtained for wildtype RCs.

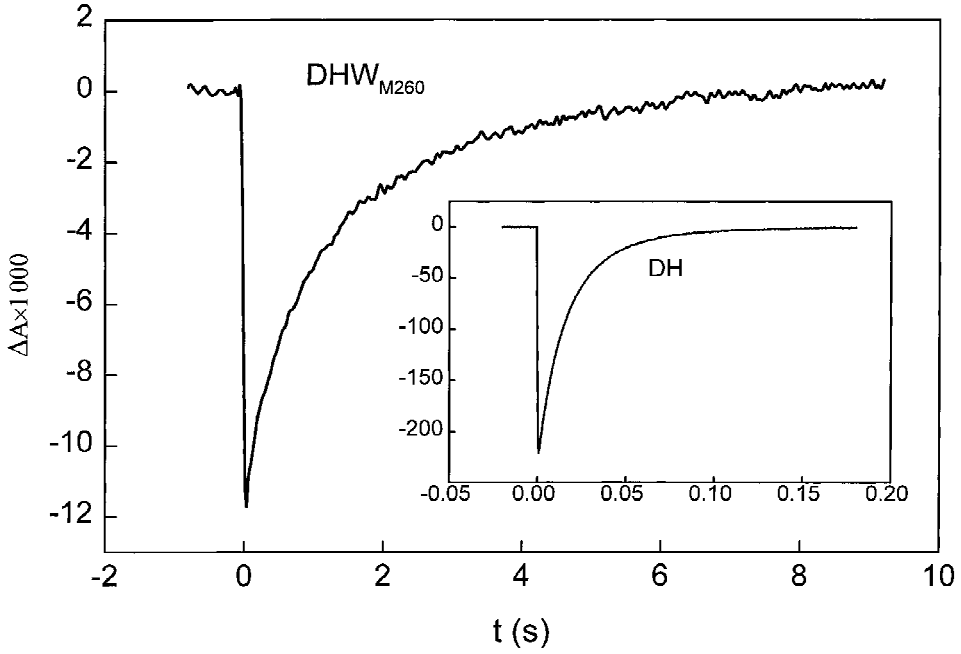

Figure 7. Charge recombination of $P^+Q_B^-$ in the DHW_{M260} mutant measured at 20 K at 890 nm. The inset shows $P^+Q_A^-$ recombination in the DH mutant, also at 20 K and at 890 nm. The samples had the same optical density at 890 nm. Note the differences in the magnitudes of the absorption changes and the time scales on which the charge-separated states recombine.

(β) instead of H_A. The increase in P* lifetime is presumably due to the lower reductive midpoint potential of bacteriochlorophyll compared to that of bacteriopheophytin, destabilizing $P^+\beta^-$ with respect to $P^+H_A^-$. The G(M203)D mutation was originally designed to add a hydrogen bond to the 9-keto carbonyl group of ring V of B_A (Williams et al. 1992a), and was expected to *raise* the B_A^-/B_A midpoint potential. Later, it was suggested (Heller et al. 1995, 1996) that the G(M203)D mutation might *lower* the B_A^-/B_A midpoint potential, possibly because of the aspartic acid residue being negatively charged (Heller et al. 1996; Czarnecki et al. 1999). On the basis of recent X-ray data, Fyfe et al. (2000) suggest alternative explanations for the increase of the P* lifetime due to the G(M203)D mutation. Wildtype RCs contain

Table 1. Characteristics of wildtype and mutant RCs of *Rba. sphaeroides* and *Rba. capsulatus* at ambient temperature

Mutation(s)	P*[a] (ps)	P/P$^+$[b] (mV)	Y[c] (%) $P^+Q_A^-$	Y[d] (%) $P^+H_B^-$	Reference
Rba. sphaeroides					
wildtype	3.2	~500	100	≤5*	Kirmaier et al (1991), Williams et al. (1992a), Lin et al. (1994)
G(M203)D	9.4	495	100		Williams et al. (1992a)
L(M214)H (β-mutant)	6.4		60		Kirmaier et al (1991)
Y(M210)W	40	552	85		Shochat et al. (1994), Nagarajan et al. (1993)
Y(M210)W/L(M214)H ($W_{M210}H$)	80		50	≤10*	This work
G(M203)D/Y(M210)W/L(M214)H ($DW_{M210}H$)	160		30	≤10*	This work
G(M203)D/(M214)H/A(M260)W (DHW_{M260})	23			≤10*	This work
L(L131)H	12.2	585	<100[e]		Williams et al. (1992a), Lin et al. (1994)
L(M160)H	5.7	565	<100[e]		Williams et al. (1992a), Lin et al. (1994)
Rba. capsulatus					
wildtype	4.3		100		Heller et al. (1996), Heller et al. (1995)
G(M201)D	7.6		100		Heller et al. (1996)
L(M212)H (β-mutant)	8.5		76		Heller et al. (1996)
G(M201)D/L(M212)H	15		70	15	Heller et al. (1996), Heller et al. (1995)

[a]P* lifetimes. [b]P/P$^+$ midpoint potentials. [c]Yield of $P^+Q_A^-$ formation. [d]Yield of $P^+H_B^-$ formation. [e]Significantly smaller than 100%, as estimated from Figure 5 in reference 2. * Upper detection limits.

a water molecule near the 9-keto carbonyl group of B_A that might form a hydrogen bond. This water molecule is not present in the X-ray structure of RCs with the G(M203)D mutation. Thus, the G(M203)D mutation may disrupt a hydrogen bond that is present in wildtype RCs and thereby destabilize $P^+B_A^-$. Alternatively, replacement of the glycine with the aspartic acid residue and removal of the water molecule may alter the local dielectric environment of the 9-keto carbonyl group.

Several hypotheses have been put forward to explain how the mutation Y(M210)W increases the P* lifetime. It was suggested that the polar hydroxyl group of the tyrosine residue may stabilize both the positive charge on P^+ and the negative charge on B_A^- (Parson et al. 1990; Alden et al. 1996) or on H_A^- (Nagarajan et al. 1993; Gunner et al. 1996). When the tyrosine is replaced with tryptophan, these stabilizations are no longer possible. An alternative explanation was provided by Ivashin et al. (1998). They suggested that replacement of tyrosine with the larger tryptophan may increase the distance between P and B_A and hence weaken the electronic coupling between these two. Recently, the X-ray crystal structure of the Y(M210)W mutant has been determined at a resolution of 2.5 Å by McAuley et al. (2000). By comparing the structures of the wildtype RC and the mutant RC, the authors found a small tilt of the macrocycle of B_A, which may weaken the interaction between P and B_A. Such a tilt is consistent with ADMR measurements by Shochat et al. (1994), who found an increased interaction between B_A and H_A. Regardless whether the increase in the lifetime of P* originates mainly from destabilization of B_A^- or from a diminished elec-

tronic coupling between P and B_A, the energetics for charge separation through the B-branch and electronic coupling between cofactors of the B-branch should be largely unaffected. No B-branch electron transfer has been reported for the Y(M210)W single mutant in the literature.

It is apparent from Figure 3 that for the $W_{M210}H$ and $DW_{M210}H$ mutants there is a significant recovery of the ground state absorption of the primary donor. The strongly increased P* lifetimes and reduced $P^+Q_A^-$ yield for these mutants as compared to wildtype RCs indicate that electron transfer through the A-branch is (partially) inhibited.

Picosecond B-branch electron transfer

In the region where H_B absorbs (the Q_x transition), only little or no bleaching (<10%) is observed on a ps timescale in both the $W_{M210}H$ and $DW_{M210}H$ mutants. This low value is surprising in view of the result obtained by Heller et al. (1995) for RCs of their G(M201)D/L(M212)H double mutant of *Rba. capsulatus*. They found a yield of 10–15% for the formation of $P^+H_B^-$ and 15% ground state recovery of P, although the P* lifetime was only 15 ps. Because our mutants have significantly longer lifetimes, we would have expected a yield of at least 15% for $P^+H_B^-$ in our triple mutant $DW_{M210}H$, as it has the mutations G(M203)D and L(M214)H, which correspond to the mutations G(M201)D and L(M212)H in the *Rba. capsulatus* mutant used by Heller et al. (1995). In actual fact we did not observe an increase of $P^+H_B^-$ formation compared to Heller et al. (1995). Instead, the increase of the P* lifetime primarily results in an increased fast recovery of the ground state of P.

A possible explanation for these contradictory results is that the B-branch of *Rba. capsulatus* is more accessible to charge separation than the B-branch of *Rba. sphaeroides*. In order to address this question we compare the characteristics of several RC mutants. They are listed in Table 1.

As mentioned, the tyrosine at position M210 is in close contact with P. Therefore, replacement of the tyrosine with tryptophan may affect the P/P^+ midpoint potential. Indeed Nagarajan et al. (1993) found that the P/P^+ midpoint potential is higher in Y(M210)W RCs than in wildtype RCs (552 and 500 mV, respectively). A similar increase of the P/P^+ midpoint potential was reported for the hydrogen bond mutant L(M160)H (Williams et al. 1992a), Table 1. The increase of the P* lifetime, however, is much larger in

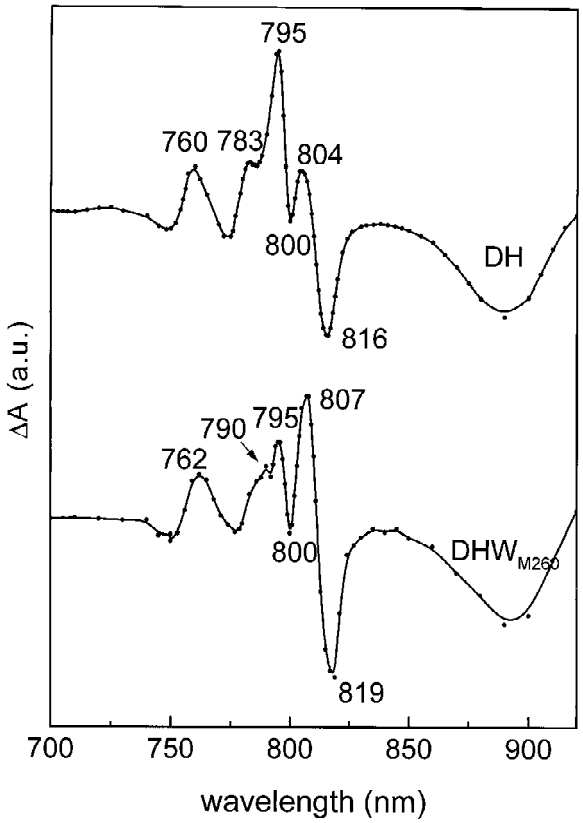

Figure 8. Absorption difference spectra at 20 K for DH and DHW_{M260} RCs. The absorption changes for the DHW_{M260} RCs were actually ~30-fold smaller than those for DH RCs.

the Y(M210)W mutant than in the L(M160)H mutant (40 and 6 ps, respectively, *versus* 3 ps for wildtype RCs), implying that the increase of the P/P^+ midpoint potential due to the Y(M210)W mutation can only partially explain the roughly tenfold increase of the P* lifetime. In turn, the increase of the P* lifetime must then be due to destabilization of $P^+B_A^-$ or $P^+H_A^-$ by the Y(M210)W mutation. A similar destabilization of $P^+B_B^-$ or $P^+H_B^-$ is unlikely because Y(M210)W is not in close contact with B_B or H_B. This argument leaves differences between the B-branches of *Rba. sphaeroides* and *Rba. capsulatus* as the only explanation why our mutants do not show appreciable electron transport through the B-branch. We note that recently Kirmaier et al. (2001) studied the YFH mutant of *Rba. capsulatus* in which the M208 tyrosine (corresponding to Y(M210) in *Rba. sphaeroides*) was swapped with the symmetry-related phenylalanine at L181, and H_A replaced by a BChl (β). This set of mutations leaves the midpoint potential of the couple P/P^+ unaffected. Swapping the residues at position M210 and

L181 would not be expected to lead to large structural changes, but the change in polarity is considerable. As mentioned, the tyrosine at position M210 may stabilize a negative charge on B_A and H_A in wildtype RCs (Parson et al. 1990; Nagarajan et al. 1993; Alden et al. 1996; Gunner et al. 1996). This stabilization is lost upon swapping the residues at M210 and L181. In turn, the newly introduced tyrosine at L181 is expected to stabilize negative charges on B_B and H_B. The lifetime of P^* of the mutant was 11 ps, compared to 8.5 and 4.3 ps for the single β-mutant and wildtype RCs, respectively. The difference in lifetime of the YFH mutant and wildtype RCs corresponds quite well with the reported branching ratio of 30% B-chain electron transport. It follows that, in agreement with the work presented here, for significant B-chain electron transport to occur one needs to destabilize the A-chain and at the same time stabilize the B-chain.

The RCs of *Rba. sphaeroides* and *Rba. capsulatus* contain the same pigments. Therefore differences between the B-branches of RCs of these species are likely due to differences in the protein subunits of the RC, in particular the L and m subunits since these bind the pigments. The L subunits of the *Rba. sphaeroides* RC and the *Rba. capsulatus* RC share 78% identical residues. Similarly 77% of the residues of the m subunits of the *Rba. sphaeroides* RC and the *Rba. capsulatus* RC are identical (Williams et al. 1984). Thus, a relatively large number of residues that are not identical in the protein subunits of the RCs of the two bacterial species may contribute to differences in their B-branches.

Differences between RCs of *Rba. sphaeroides* and *Rba. capsulatus* may also be induced by their isolation. For *Rba. capsulatus* RCs, the position of the absorption band of P at 865 nm tends to shift to 850 nm during the purification procedure (Prince and Youvan 1987). This shift suggests structural changes in the RC. It would be interesting to see whether the yield of $P^+H_B^-$ formation is related to the position of the long-wavelength band of P.

The primary photochemistry in the *Rba. sphaeroides* DHW_{M260} mutant would be expected to be similar to that in the *Rba. capsulatus* DH mutant (Heller et al. 1995) assuming that the mutation A(M260)W does not affect the transfer of an electron from P^* to B_A or β. In the DHW_{M260} mutant P^* decay is best fitted with two exponential components with time constants of 2.5 (40%) and 36 ps (60%). A monoexponential fit of the P^* decay in DH RCs of *Rba. capsulatus* yielded 15 ps (Heller et al. 1995), corresponding quite well with our average time constant of 23 ps. As was reported for the *Rba. capsulatus* DH mutant (Heller et al. 1995), there is significant ground state recovery during the decay of P^*. In contrast, a higher yield for $P^+H_B^-$ formation was reported for the *Rba. capsulatus* DH mutant (15%) than found here for the DHW_{M260} RC. Thus, it appears that electron transfer through the B-branch of the *Rba. sphaeroides* RC is more difficult than through that of *Rba. capsulatus* RCs. The rate constant of B-branch electron transfer in principle can be derived by combining information on the lifetime of P^* and the yield of $P^+H_B^-$. The uncertainties in both lifetime (mono, bi-, or multiexponential?) and yield, however, make such an estimate difficult and therefore a quantitative comparison between *Rba. sphaeroides* and*Rba. capsulatus* hazardous.

(Milli)second absorption difference spectroscopy of the DHW_{M260} mutant

The DHW_{M260} mutant is similar to the*Rba. capsulatus* DHV mutant described by Laible et al. (1998). The mutants differ mainly in the manner by which Q_A-less RCs are obtained. In the *Rba. capsulatus* DHV mutant the affinity of ubiquinone is weaker for the Q_A site than for the Q_B site due to the W(M250)V mutation. Purified DHV RCs are devoid of both Q_A and Q_B. Because of the higher affinity of quinone for the Q_B site, RCs that contain preferentially Q_B can be obtained by the addition in a controlled manner of small amounts of ubiquinone to the purified RCs. It is difficult, however, to obtain in this way Q_B-containing RCs completely devoid of Q_A. In our *Rba. sphaeroides* DHW_{M260} mutant the bulky side chain of the tryptophan residue introduced by the A(M260)W mutation protrudes into the Q_A binding pocket and thereby rigorously excludes the binding of quinone in the Q_A binding site (Ridge et al. 1999; McAuley et al. 1999, 2000).

Small transient signals were observed in the (milli)second range for the DHW_{M260} mutant at both room temperature and at 20 K. Several lines of evidence suggest that these signals are due to formation and recombination of $P^+Q_B^-$ and not of $P^+Q_A^-$: (1) no Q_A is present in our samples due to the A(M260)W mutation; (2) the signals at room temperature disappear upon addition of terbutryn, a well-known competitive inhibitor of UQ_{10} for the Q_B site, but not of UQ_{10} in the Q_A site. The small signal remaining (Figure 6) is due to incomplete inhibition of the Q_B site. It decays in the seconds range, not in ms as would

$P^+Q_A^-$; (3) biphasic recombination at 20 K (0.6 and 2.7 s) is much slower than what is normally found for $P^+Q_A^-$ recombination in wildtype RCs (30 ms) or in *Rba. sphaeroides* DH RCs at cryogenic temperatures (see Figure 7). The latter observation makes it unlikely that the transient signals are due to $P^+Q_A^-$ formation in a small fraction of RCs that contain Q_A, despite the A(M260)W mutation. Finally, the absorption difference spectra obtained for the DH and DHW_{M260} mutants of the *Rba. sphaeroides* RC at 20 K (Figure 8) are different, presumably because they represent absorption changes due to $P^+Q_A^-$ and $P^+Q_B^-$ decay, respectively. Apparently, in contrast to wildtype RCs where $P^+Q_B^-$ is not observed at low temperatures (Parson 1978), $P^+Q_B^-$ can be formed at 20 K in DHW_{M260}. In wildtype RCs $P^+Q_B^-$ formation proceeds via the A-branch; at low temperatures electron transfer leads solely to the formation of $P^+Q_A^-$, and further electron transfer to Q_B does not occur (Parson 1978). That $P^+Q_B^-$ can be formed at 20 K in the DHW_{M260} mutant, which lacks Q_A, suggest that in this mutant $P^+Q_B^-$ formation occurs by a different mechanism. Although transient bleaching of H_B due to its photoreduction could not be unequivocally demonstrated, presumably due to the low yield of $P^+H_B^-$ formation in combination with an unfavorable signal–noise ratio, we suggest that $P^+Q_B^-$ formation in the DHW_{M260} mutant occurs via the B-branch.

Charge recombination at room temperature from $P^+Q_B^-$ in the DHW_{M260} mutant (two exponential decay components of 4.5 and 57 s with equal amplitudes) is much slower than in wildtype RCs (with a decay component of 1 s (Okamura et al. 1982)). The average time constant of 30 s corresponds quite well to the time constant of 25 s found by Takahashi and Wraight (1992) for charge recombination of $P^+Q_B^-$ in RCs of *Rba. sphaeroides* with the D(L213)N mutation. This mutation near Q_B increases the equilibrium constant of $P^+Q_A^-Q_B$ and $P^+Q_AQ_B^-$, favoring formation of the latter. Takahashi and Wraight (1992) and Labahn et al. (1994) suggested that in this mutant charge recombination from $P^+Q_B^-$ occurs via the *direct* pathway, which only involves cofactors of the B-branch. In contrast, in wildtype RCs $P^+Q_B^-$ recombines mainly by the *indirect* pathway. This pathway involves transient formation of $P^+Q_A^-$ and subsequent charge recombination from this state (Kleinfeld et al. 1984a). $P^+Q_B^-$ recombination cannot occur by the *indirect* mechanism in DHW_{M260} RCs since they do not contain Q_A.

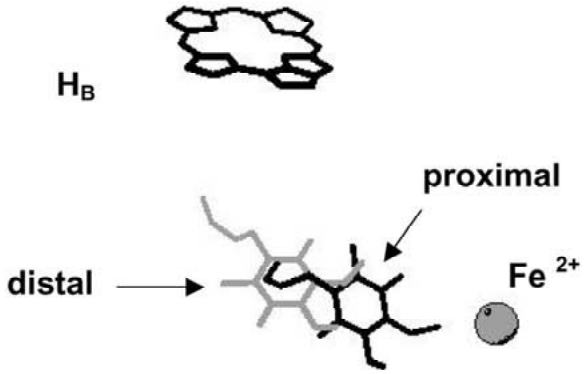

Figure 9. Schematic representation of UQ_{10} in the Q_B binding pocket showing the distal and proximal sites with respect to the iron. For clarity, only the porphyrin ring of H_B is shown and most of the isoprenoid tail of the UQ_{10} molecules has been omitted. The picture was drawn after Stowell et al. (1997) using the Molscript program (Kraulis 1991).

As mentioned, at cryogenic temperatures electron transfer from Q_A to Q_B does not proceed. It is possible, however, to trap the state $P^+Q_B^-$ in wildtype RCs by cooling them under illumination. In this case, a very slow recombination is observed (a time constant of 2×10^5 s at 18 K) and after recombination the state $P^+Q_B^-$ can be reformed with illumination at cryogenic temperatures (Kleinfeld et al. 1984b). The enormous difference in $P^+Q_B^-$ lifetimes in our DHW_{M260} mutant and in wildtype RCs suggests that there are differences in the conformation of the respective RCs. A likely explanation is provided by Stowell et al. (1997) who found different positions for Q_B and Q_B^- in wildtype RCs in crystals frozen in the dark and in the light, respectively. In RCs in the dark Q_B is in a distal position with respect to the ferrous iron ion (see Figure 9), whereas inthe reduced form (Q_B^-) it is in a proximal position with respect to the iron ion. It was postulated that Q_B has to move from the distal to the proximal site for electron transfer from Q_A^- to Q_B. When $P^+Q_B^-$ is trapped in these RCs by cooling under illumination from room temperature to 77 K, Q_B^- presumably stays in the proximal position. When RCs are frozen in the dark, Q_B is not able to move from the distal to the proximal site so that it cannot accept an electron from Q_A. In contrast, in DHW_{M260} RCs reduction of Q_B probably occurs via the B-branch. Q_B is likely to accept an electron from H_B^- when it is in the distal site, which is closer to H_B. Thus, the differences in the charge recombination times in wildtype and DHW_{M260} RCs at cryogenic temperatures are probably related to different posi-

tions of Q_B. Recently, evidence was obtained that in single crystals of the A(M260)W mutant RCs, Q_B is not located in the distal position in the dark as in R26 RCs (Stowell et al. 1997), but in the proximal position (McAuley et al. 2000). Assuming that H_B^- cannot transfer electrons to Q_B in the proximal position and that on average 3% of Q_B is bound to the distal site, this observation would explain our low yield of $P^+Q_B^-$ formation in a single flash (3%) and our inability to photoaccumulate $P^+Q_B^-$. The same argument may explain why charge recombination from $P^+Q_B^-$ is much faster at 20 K (time constants of 0.6 and 2.7 s) than at room temperature (time constants of 4.5 and 57 s). At 20 K, Q_B in the DHW_{M260} mutant is unlikely to move from the distal site to the proximal site after accepting an electron. Such a movement may be possible, however, at room temperature. In that case, it would be in the same position as in the D(L213)N mutant. The similar recombination times for $P^+Q_B^-$ recombination in the DHW_{M260} mutant and the D(L213)N mutant can be accounted for if in both mutants recombination occurs by the *direct* pathway, possibly involving a movement of Q_B^- from the strongly binding proximal site to the weakly binding distal site to deliver an electron to H_B.

It should be noted that most of the evidence for the formation of $P^+Q_B^-$ described so far has been obtained by studying absorption difference kinetics of the primary donor. We have searched for EPR signals due to Q_B^- in order to corroborate the optical evidence for $P^+Q_B^-$ formation. However, no signals were found. In wildtype RCs, both Q_A^- and Q_B^- are magnetically coupled to the ferrous iron ion, giving rise to broad signals centered near g = 1.8 (Feher and Okamura 1978). No such signals were found in the DHW_{M260} mutant. However, since in the DHW_{M260} mutant Q_B^- may be formed in the distal site it may not be coupled to the iron. In this case, a signal near g = 2.0046 may be expected, as is found for Q_A^- when it is not coupled to the iron (Feher and Okamura 1978). However, no signal of Q_B^- was found here either, or at any intermediate g-value. Our inability to detect any EPR signals due to Q_B^- is probably due to the low yield of $P^+Q_B^-$ formation after a single saturating flash (3%). As for the optical experiment we did not succeed in photoaccumulating the EPR signal of Q_B^-.

Conclusions

Guided by the notion that mutants with long P* lifetimes would be candidates for increased B-branch electron transfer, we have constructed the new double mutant Y(M210)W/L(M214)H and the new triple mutant G(M203)D/Y(M210)W/L(M214)H of *Rba. sphaeroides* with P* lifetimes in isolated RCs of 80 and 160 ps, respectively, compared to 3 ps for wildtype RCs. In these mutants, electron transfer through the A-branch is partially inhibited as indicated by the reduced yields for $P^+Q_A^-$ on a ns timescale (50 and 30%, respectively). In spite of the very long P* lifetimes in our mutants, no significant (<10%) B-branch electron transfer is observed. Inhibition of electron transfer primarily leads to recovery of the ground state.

To investigate the possible reduction of Q_B on a (milli)second timescale we have constructed the triple mutant G(M203)D/L(M214)H/A(M260)W in which Q_A binding is inhibited. The P* decay of the triple mutant is biphasic with an average lifetime of 23 ps. We find a yield of no more than $3 \pm 0.5\%$ for $P^+Q_B^-$ formation in a single flash. Photoaccumulation at cryogenic temperatures was not possible. From the flash-induced signal of $P^+Q_B^-$ at 20 K we have constructed the first low-temperature $P^+Q_B^-$ absorption difference spectrum. It differs from that of $P^+Q_A^-$ mainly by the electro-optical effect on the absorption bands of B_A and B_B resulting from the charge on the quinone.

Our results strongly suggest that in the *Rba. sphaeroides* RC no appreciable B-branch electron transfer can be obtained by just inhibiting electron transfer through the A-branch.

Acknowledgements

We are indebted to Mr I.V. Borovykh for carrying out the EPR experiments and to A.H.M. de Wit for his help in growing the bacteria. HPP and RdW acknowledge support from the Chemistry Division of the Netherlands Organization for Scientific Research (NWO).

References

Alden RG, Parson WW, Chu ZT and Warshel A (1996) Orientation of the OH dipole of Tyrosine (M)210 and its effect on electrostatic energies in photosynthetic bacterial reaction centers. J Phys Chem 100: 16761–16770

Allen JP, Feher G, Yeates TO, Komiya H and Rees DC (1987a) Structure of the reaction center from *Rhodobacter sphaeroides* R-26: the cofactors. Proc Natl Acad Sci USA 84: 5730–5734

Allen JP, Feher G, Yeates TO, Komiya H and Rees DC (1987b) Structure of the reaction center from *Rhodobacter sphaeroides* R-26: the protein subunits. Proc Natl Acad Sci USA 84: 6162–6166

Allen JP, Feher G, Yeates TO, Komiya H and Rees DC (1988a) Structure of the reaction center from *Rhodobacter sphaeroides* R-26: protein-cofactor (quinones and Fe^{2+}) interactions. Proc Natl Acad Sci USA 85: 8487–8491

Allen JP, Feher G, Yeates TO, Komiya H and Rees DC (1988b) Structure of the reaction center from *Rhodobacter sphaeroides* R-26 and 2.4.1. In: Breton J and Verméglio A (eds) The Photosynthetic Bacterial Reaction Center. Structure and dynamics, pp 5–11. Plenum Press, New York

Aumeier W, Eberl U, Ogrodnik A, Volk M, Scheidel G, Feick R, Plato M and Michel-Beyerle M-E (1990) Unidirectionality of charge separation in reaction centers of *Rba. sphaeroides* and *Chloroflexus aurantiacus*. In: Baltscheffsky M (ed) Current Research in Photosynthesis, Vol I, pp 133–136. Kluwer Academic Publishers, Dordrecht, The Netherlands

Bixon M, Jortner J, Michel-Beyerle M-E and Ogrodnik A (1989) A superexchange mechanism for the primary charge separation in photosynthetic reaction centers. Biochim Biophys Acta 977: 273–286

Bosch M K (1995). Primary photochemistry in photosynthetic reaction centers. A cw and pulsed EPR study. Dissertation, Leiden University, Leiden, The Netherlands

Czarnecki K, Kirmaier C, Holten D and Bocian DF (1999) Vibrational and photochemical consequences of an Asp residue near the photoactive accessory bacteriochlorophyll in the photosynthetic reaction center. J Phys Chem A 103: 2235–2246

Chirino AJ, Lous EJ, Huber M, Allen JP, Schenck CC, Paddock ML, Feher G and Rees DC (1994) Crystallographic analyses of site-directed mutants of the photosynthetic reaction center from *Rhodobacter sphaeroides*. Biochemistry 33: 4584–4593

Dzuba SA, Proskuryakov II, Hulsebosch RJ, Bosch MK, Gast P and Hoff AJ (1996) Control of radical pair lifetimes by microwave irradiation: Application to photosynthetic reaction centres. Chem Phys Lett 253: 361–366

Ermler U, Fritzsch G, Buchanan SK and Michel H (1994) Structure of the photosynthetic reaction centre from *Rhodobacter sphaeroides* at 2.65 Å resolution: cofactors and protein–cofactor interactions. Structure 2: 925–936

Feher G and Okamura MY (1978) Chemical composition and properties of reaction centers. In: Clayton RK and Sistrom WR (eds) The Photosynthetic Bacteria, pp 349–386. Plenum Press, New York/London

Franken EM (1997) Primary processes and electron transfer in anoxygenic photosynthetic bacteria. Dissertation, Leiden University, Leiden, The Netherlands

Fyfe PK, Ridge JP, McAuley KE, Cogdell RJ, Isaacs NW and Jones MR (2000) Structural consequences of the replacement of glycine M203 with aspartic acid in the reaction center from *Rhodobacter sphaeroides*. Biochemistry 39: 5953–5960

Goldsmith JO and Boxer SG (1996) Rapid isolation of bacterial photosynthetic reaction centers with an engineered poly-histidine tag. Biochim Biophys Acta 1276: 171–175

Gunner MR, Nicholls A and Honig B (1996) Electrostatic potentials in *Rhodopseudomonas viridis* reaction centers: implications for the driving force and directionality of electron transfer. J Phys Chem 100: 4277–4291

Hartwich G, Bieser G, Langenbacher T, Müller P, Richter M, Ogrodnik A, Scheer H and Michel-Beyerle M-E (1997) B-branch electron transfer in bacterial photosynthetic reaction centers by energetically activating A-branch charge separation. Biophys J 72: A8-E7

Hartwich G, Müller P, Richter M, Bieser G, Ogrodnik A, Scheer H and Michel-Beyerle M-E (1998) Activating A-branch electron transfer in bacterial photosynthetic reaction centers imposes B-branch charge separation. XIth International Congress on Photosynthesis (Budapest). Abstr, p 51

Heller BA, Holten D and Kirmaier C (1995) Control of electron transfer between the L- and M-sides of photosynthetic reaction centers. Science 269: 940–945

Heller BA, Holten D and Kirmaier C (1996) Effects of Asp residues near the L-side pigments in bacterial reaction centers. Biochemistry 35: 15418–15427

Hoff AJ (1988). Nomen est omen. A note on nomenclature. In: Breton, J and Verméglio A (eds) The Bacterial Photosynthetic Center: Structure and Dynamics, pp 98–99. Plenum Press, New York

Huber H, Meyer M, Nagele T, Hartl I, Scheer H, Zinth W and Wachtveitl J (1995) Primary photosynthesis in reaction centers containing four different types of electron accepters at site H_A. Chem Phys 197: 297–305

Ivashin N, Kallebring B, Larsson S and Hansson O (1998) Charge separation in photosynthetic reaction centers. J Phys Chem B 102: 5017–5022

Katilius E, Turanchik T, Lin S, Taguchi AKW and Woodbury NW (1999) B-side electron transfer in a *Rhodobacter sphaeroides* reaction center mutant in which the B-side monomer bacteriochlorophyll is replaced with bacteriopheophytin. J Phys Chem B 103: 7386–7389

Kennis JTM, Streltsov AM, Aartsma TJ, Nozawa T and Amesz J (1996) Energy transfer and exciton coupling in isolated B800-850 complexes of the photosynthetic purple sulfur bacterium *Chromatium tepidum*. The effect of structural symmetry on bacteriochlorophyll excited states. J Phys Chem 100: 2438–2442

Kennis JTM, Shkuropatov AY, van Stokkum IHM., Gast P, Hoff AJ, Shuvalov VA and Aartsma TJ (1997a) Formation of a long-lived $P^+B_A^-$ state in plant pheophytin-exchanged reaction centers of *Rhodobacter sphaeroides* R26 at low temperature. Biochemistry 36: 16231–16238

Kennis JTM, Streltsov AM, Permentier H, Aartsma TJ and Amesz J (1997b) Exciton coherence and energy transfer in the LH2 antenna complex of *Rhodopseudomonas acidophila* at low temperature. J Phys Chem B 101: 8369–8374

Kirmaier C, Holten D and Parson WW (1985a) Temperature and detection-wavelength dependence of the picosecond electron-transfer kinetics measured in *Rhodopseudomonas sphaeroides* reaction centers. Resolution of new spectral and kinetic components in the primary charge-separation process. Biochim Biophys Acta 810: 33–48

Kirmaier C, Holten D and Parson WW (1985b) Picosecond-photodichroism studies of the transient states in *Rhodopseudomonas sphaeroides* reaction centers at 5 K. Effects of electron transfer on the six bacteriochlorin pigments. Biochim. Biophys. Acta 810: 49–61

Kirmaier C, Gaul D, DeBey R, Holten D and Schenck CC (1991). Charge separation in a reaction center incorporating bacteriochlorophyll for photoactive bacteriopheophytin. Science 251: 922–927

Kirmaier C, Weems D, and Holten D (1999) M-side electron transfer in reaction center mutants with a lysine near the nonphotoactive bacteriochlorophyll. Biochemistry 38: 11516–11530

Kirmaier C, He C and Holten D (2001) Manipulating the direction of electron transfer in the bacterial reaction center by swapping

Phe for Tyr near $BChl_M$ (L181) and Tyr for Phe near $BChl_L$ (M208). Biochemistry 40: 12132–12139

Kleinfeld D, Okamura MY and Feher G (1984a) Electron transfer in reaction centers of *Rhodopseudomonas sphaeroides*. I. Determination of the charge recombination pathway of $D^+Q_AQ_B^-$ and free energy and kinetic relations between $Q_A^-Q_B$ and $Q_AQ_B^-$. Biochim Biophys Acta 766: 126–140

Kleinfeld D, Okamura MY and Feher G (1984b) Electron-transfer kinetics in photosynthetic reaction centers cooled to cryogenic temperatures in the charge-separated state: evidence for light-induced structural changes. Biochemistry 23: 5780–5786

Kraulis PJ (1991). Molscript: A program to produce both detailed and schematic plots of protein structures. J Appl Cryst 24: 946–950

Labahn A, Paddock ML, McPherson PH, Okamura MY and Feher G (1994) Direct charge recombination from $D^+Q_AQ_B^-$ to DQ_AQ_B in bacterial reaction centers from *Rhodobacter sphaeroides* J Phys Chem 98: 3417–3423

Laible PD, Kirmaier C, Holten D, Tiede D, Schiffer M and Hanson DK (1998) Formation of $P^+Q_B^-$ via B-branch electron transfer in mutant reaction centers. In: Garab G (ed) Photosynthesis: Mechanisms and Effects, Vol II, pp 849–852. Kluwer Academic Publishers, Dordrecht, The Netherlands

Landt O, Grunert H-P and Hahn U (1990) A general method for rapid site-directed mutagenesis using the polymerase chain reaction. Gene 96: 125–128

Lin X, Murchison HA, Nagarajan V, Parson WW, Allen JP and Williams JC (1994) Specific alteration of the oxidation potential of the electron donor in reaction centers from *Rhodobacter sphaeroides*. Proc Natl Acad Sci USA 91: 10265–10269

McAuley-Hecht KE, Fyfe PK, Ridge JP, Prince SM, Hunter CN, Isaacs NW, Cogdell RJ, and Jones, MR (1998) Structural studies of wild-type and mutant reaction centers from an antenna-deficient strain of *Rhodobacter sphaeroides*: monitoring the optical properties of the complex from bacterial cell to crystal. Biochemistry 37: 4740–4750

McAuley KE, Fyfe PK, Ridge JP, Isaacs NW, Cogdell RJ and Jones MR (1999) Structural details of an interaction between cardiolipin and an integral membrane protein. Proc Natl Acad Sci USA 96: 14706–14711

McAuley KE, Fyfe PK, Ridge JP, Cogdell RJ, Isaacs NW and Jones MR (2000) Ubiquinone binding, ubiquinone exclusion, and detailed cofactor conformation in a mutant bacterial reaction center. Biochemistry 39: 15032–15043

Meyer M and Scheer H (1995) Reaction centers of *Rhodobacter sphaeroides* R26 containing C-3 acetyl and vinyl (bacterio)pheophytins at sites H_A,H_B. Photosynth Res 44: 55–65

Murchison HA, Alden RG, Allen JP, Peloquin JM, Taguchi AK, Woodbury NW and Williams JC (1993) Mutations designed to modify the environment of the primary electron donor of the reaction center from *Rhodobacter sphaeroides*: Phenylalanine to leucine at L167 and histidine to phenylalanine at L168. Biochemistry 32: 3498–3505

Nagarajan V, Parson WW, Davis D and Schenck CC (1993) Kinetics and free energy gaps of electron-transfer reactions in *Rhodobacter sphaeroides* reaction centers. Biochemistry 32: 12324–12336

Okamura MY, Debus RJ, Kleinfeld D and Feher G (1982) Quinone binding sites in reaction centers from photosynthetic bacteria. In: Trumpower BL (ed) Function of Quinones in Energy Conserving Systems, pp 299–317. Academic Press, New York

Otte SCM (1992) Pigment systems of photosynthetic bacteria and Photosystem II of green plants. Dissertation, Leiden University, Leiden, The Netherlands

Paddock ML, Rongey SH, Feher G and Okamura MY (1989) Pathway of proton transfer in bacterial reaction centers: Replacement of glutamic acid 212 in the L subunit by glutamine inhibits quinone (secondary acceptor) turnover. Proc Natl Acad Sci USA 86: 6602–6606

Parson WW (1978) Quinones as secondary electron acceptors. In: Clayton RK and Sistrom WR (eds) The Photosynthetic Bacteria, pp 349–386. Plenum Press, New York/London

Parson WW, Chu ZT and Warshel A (1990) Electrostatic control of charge separation in bacterial photosynthesis. Biochim Biophys Acta 1017: 251–272

Prince RC and Youvan DC (1987) Isolation and spectroscopic properties of photochemical reaction centers from *Rhodobacter capsulatus*. Biochim Biophys Acta 890: 286–291

Ridge JP, van Brederode ME, Goodwin MG van Grondelle R and Jones MR (1999) Mutations that modify or exclude binding of the Q_A ubiquinone and carotenoid in the reaction center from *Rhodobacter sphaeroides*. Photosynth Res 59: 9–26

Robles SJ, Breton J and Youvan DC (1990) Partial symmetrization of the photosynthetic reaction center. Science 248: 1402–1405

Sambrook J, Fritsch EF and Maniatis T (1989) Molecular Cloning: A Laboratory Manual. Cold Spring Harbor Laboratory Press, Cold Spring Harbor, New York

Schmidt S, Arlt T, Hamm P, Huber H, Nagele T, Wachtveitl J, Zinth W, Meyer M and Scheer H (1995) Primary electron-transfer dynamics in modified bacterial reaction centers containing pheophytin-a instead of bacteriopheophytin-a. Spectrochim. Acta A 51: 1565–1578

Shochat S, Arlt T, Francke C, Gast P, Van Noort PI, Otte SCM, Schelvis HPM, Schmidt S, Vijgenboom E, Vrieze J, Zinth W and Hoff AJ (1994) Spectroscopic characterization of reaction centers of the (M)Y210W mutant of the photosynthetic bacterium *Rhodobacter sphaeroides*. Photosynth Res 40: 55–66

Shochat S, Gast P, Hoff AJ, Boender GJ, van Leeuwen S, van Liemt WBS, Vijgenboom E, Raap J, Lugtenburg J and de Groot HJM (1995) C-13 MAS NMR evidence for a homogeneously ordered environment of Tyrosine-M210 in reaction centres of *Rhodobacter sphaeroides*. Spectrochim Acta A 51: 135–144

Simon R, Preifer U and Pühler A (1983) A broad host range mobilization system for in vivo genetic engineering: transposon mutagenesis in Gram negative bacteria. Biotechnology 1: 784–791

Sistrom WR (1977) Transfer of chromosomal genes mediated by plasmid R68.45 in *Rhodopseudomonas sphaeroides*. J Bacteriol 131: 526–532

Stocker JW, Taguchi AK, Murchison HA, Woodbury NW and Boxer SG (1992) Spectroscopic and redox properties of sym1 and (M)F195H: *Rhodobacter capsulatus* reaction center symmetry mutants which affect the initial electron donor. Biochemistry 31: 10356–10362

Stowell MH, McPhillips TM, Rees DC, Soltis SM, Abresch E and Feher G (1997) Light-induced structural changes in photosynthetic reaction center: implications for mechanism of electron-proton transfer. Science 276: 812–816

Takahashi E and Wraight CA (1992) Proton and electron transfer in the acceptor quinone complex of *Rhodobacter sphaeroides* reaction centers: characterization of site-directed mutants of the two ionizable residues, GluL212 and AspL213, in the Q_B binding site. Biochemistry 31: 855–866

Tang CK, Williams JC, Taguchi AK, Allen JP and Woodbury NW (1999) $P^+H_A^-$ charge recombination reaction rate constant in *Rhodobacter sphaeroides* reaction centers is independent of the P/P^+ midpoint potential. Biochemistry 38: 8794–8799

Tiede DM, Kellogg E and Breton J (1987) Conformational changes following reduction of the bacteriopheophytin electron acceptor in reaction centers of *Rhodopseudomonas viridis*. Biochim Biophys Acta 892: 294–302

Visser JWM (1975) Photosynthetic reactions at low temperatures. Dissertation, Leiden University, Leiden, The Netherlands

Volk M, Scheidel G, Ogrodnik A, Feick R and Michel–Beyerle ME (1991) High quantum yield of charge separation in reaction centers of *Chloroflexus aurantiacus*. Biochim Biophys Acta 1058: 217–224

Williams JC, Steiner LA, Feher G and Simon MI (1984) Primary structure of the L subunit of the reaction center from *Rhodopseudomonas sphaeroides*. Proc Natl Acad Sci USA 81: 7303–7307

Williams JC, Alden RG, Murchison HA, Peloquin JM, Woodbury NW and Allen JP (1992a) Effects of mutations near the bacteriochlorophylls in reaction centers from *Rhodobacter sphaeroides*. Biochemistry 31: 11029–11037

Williams JC, Woodbury NW, Taguchi AKW, Peloquin JM, Murchison HA, Alden RG and Allen JP (1992b) Mutations that affect the donor midpoint potential in reaction centers from *Rhodobacter sphaeroides*. In: Breton J and Verméglio A (eds) The Photosynthetic Bacterial Reaction Center II, pp 25–31. Plenum Press, New York

Woodbury NW and Allen JP (1995) The pathway, kinetics and thermodynamics of electron transfer in wild type and mutant reaction centers of purple nonsulfur bacteria. In: Blankenship RE, Madigan MT and Bauer CE (eds) Anoxygenic Photosynthetic Bacteria, pp 527–557. Kluwer Academic Publishers, Dordrecht, The Netherlands

Yanish-Perron C, Viera J and Messing J (1985) Improved M13 phage cloning vectors and host strains: Nucleotide sequences of the M13 mp18 and pUC19 vectors. Gene 33: 103–119